Lawrence Berkeley National Laboratory
LBL Publications

Title
Optimization of a p-Coumaric Acid Biosensor System for Versatile Dynamic Performance.

Permalink
https://escholarship.org/uc/item/9482g3nh

Journal
ACS Synthetic Biology, 10(1)

Authors
Jiang, Tian
Yan, Yajun
Li, Chenyi

Publication Date
2021-01-15

DOI
10.1021/acssynbio.0c00500

Peer reviewed

eScholarship.org Powered by the California Digital Library
University of California

Author Manuscript
Author Manuscript
Author Manuscript
Author Manuscript

HHS Public Access
Author manuscript
ACS Synth Biol. Author manuscript; available in PMC 2022 January 15.

Published in final edited form as:
ACS Synth Biol. 2021 January 15; 10(1): 132–144. doi:10.1021/acssynbio.0c00500.

Optimization of a *p*-coumaric acid biosensor system for versatile dynamic performance

Tian Jiang[1], **Chenyi Li**[1], **Yajun Yan**[1,*]

[1]School of Chemical, Materials, and Biomedical Engineering, College of Engineering, The University of Georgia, Athens, GA 30602, USA

Abstract

Metabolic engineering is a promising approach for the synthesis of valuable compounds. Transcriptional factor-based biosensors are efficient tools to regulate the metabolic pathway dynamically. Here, we engineered the *p*-coumaric acid responsive regulator PadR from *Bacillus subtilis.* We found that *yveF* and *yveG* , two previously uncharacterized components in the sensor system, showed positive impacts on the regulation of PadR-P_{padC} sensor system, mostly on assisting the release of the repression by PadR. By site directed PadR engineering, we obtained two mutants, K64A and H38A, which exhibited increased dynamic range and superior sensitivity. To increase the promoter strength of the sensor system and investigate whether the PadR binding boxes can function in a “plug-and-play” manner, a series of hybrid promoters were constructed. Four of them P1, P2, P7, and P9 showed increased strength compared to P_{padC} and can be regulated by PadR and *p*-coumaric acid. The PadR variants and hybrid promoters obtained in this paper would expand the applicability of this sensor system ./in future metabolic engineering research.

Graphical Abstract

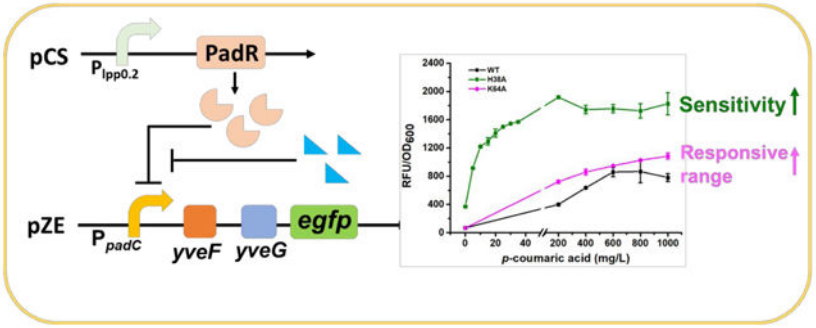

Keywords

PadR; *p*-coumaric acid; hybrid promoter; biosensor

[*]**Corresponding Authors**: yajunyan@uga.edu. Phone: +1-706-542-8293.

Author Contributions

T.J. and C.L. performed the experiments. T.J. wrote the manuscript. T.J., C.L. and Y.Y. revised the manuscript. Y.Y. directed the research.

The authors declare no competing financial interest.

Author Manuscript Author Manuscript Author Manuscript Author Manuscript

Introduction

Metabolic engineering is a sustainable and promising approach for the synthesis of various compounds, such as natural products[1, 2], pharmaceuticals[3], biofuels[4], and bulk chemicals[5, 6]. It can be achieved by combining heterologous or non-natural biosynthetic pathways into genetically advantageous microbial cell factories. In these processes, metabolic imbalance and toxic intermediates can affect the cell growth and final productivity. To address this problem, transcriptional factor-based biosensor can be used to dynamically regulate gene expression and release the burden from unbalanced metabolism. To date, transcriptional factor-based biosensors have been widely applied in dynamic regulation for the synthesis of muconic acid[7], fatty acids[8], and other valuable compounds[9–11]. In addition to the application in dynamic pathway regulation, transcriptional factor-based biosensors also were applied for high-throughput screening, which were demonstrated efficient for screening high-yield strains of 1-butanol[12], ectoine[13], benzoic acid, L-phenylalanine, and malonyl-CoA[14]. While the progress was promising, there are some challenges when utilizing transcriptional factor-based biosensors in metabolic engineering, such as poor substrate specificity, sub-optimal output strength, or narrow dynamic range. Fundamental research focusing on characterization of biosensors and studies on engineering the biosensor systems to increase their usability are thus essential to expand their application in metabolic engineering.

PadR is a transcriptional repressor which can inhibit the expression of phenolic acid decarboxylase (PadC) in *Bacillus subtilis* by binding to the −10 region in P_{padC} (the promoter of *padC* gene) and blocking the access of RNA polymerase. When *Bacillus subtilis* is exposed to the environment containing *p*-coumaric acid or ferulic acid, these compounds can bind to PadR and cause conformational change in this repressor, releasing the inhibition. (Fig.1)[15, 16]. The PadR-P_{padC} biosensor system can be applied in high-throughput screening for strains with increased *p*-coumaric acid or ferulic acid titer[17]. Besides, it shows potential in dynamic regulation to control the synthesis of flavonoids and polyphenols, which are the derivates of *p*-coumaric acid or ferulic acid. Both flavonoids and polyphenols are valuable natural products, and the market sizes of flavonoids and polyphenols are predicted to be $1.06 billion and $2.08 billion by 2025, respectively. In recent years, researchers paid lots of attention on PadR-P_{padC} biosensor system. Sung-il Yoon and coworkers obtained the crystal structure of PadR and its complex with specific DNA sequence, which revealed the key residues affecting the binding between PadR and P_{padC} and provided valuable insights for PadR optimization[18]. To apply this biosensor system in high-throughput screening, Haakan N. Joensson and colleagues applied RBS engineering to fine-tune the expression level of PadR and increased the dynamic range of the PadR-P_{padC} biosensor system. The optimized biosensor was then applied to screen yeast variants with high *p*-coumaric acid titer[17]. However, some key regulation components of this system have not been fully characterized yet. For example, there are two hypothetic genes, *yveF* and *yveG*, located in the intergenic region between the P_{padC} and *padC* gene. The specific functions of these two hypothetic genes in the aspect of PadR regulation have not been characterized. Besides, even though the key residues of PadR were reported, how the mutations of these residues affect the dynamic performance of the biosensor system have not been explored and characterized. Moreover,

Author Manuscript Author Manuscript Author Manuscript Author Manuscript

the narrow dynamic range, which caused by strong binding affinity between PadR and corresponding promoter sequences, limited its application in metabolic engineering.

In this paper, we cloned PadR and P_{padC} from *Bacillus subtilis.* Through functional analysis and verification, we characterized that the addition of *yveF* and *yveG* strongly enhanced the dynamic range of this biosensor system, which largely expanded its usability and potential application in metabolic engineering. The expression level of PadR on the dynamic range of this biosensor was also systematically analyzed. Then, we investigated the key residues affecting the binding between PadR and P_{padC} and obtained a PadR single mutant (K64A) which exhibited an increased operational range (0–1000 mg/L) induced by *p*-coumaric acid compared with the wild type PadR (0–600 mg/L). Besides, another PadR single mutant H38A exhibited the increased sensitivity and strength compared wild type PadR. To increase the promoter strength and investigate whether the PadR binding boxes can function in a "plug-and-play" manner, we designed a series of hybrid promoters by placing the PadR binding boxes into the strong constitutive promoter PL with or without *yveF* and *yveG*. By doing this, we demonstrated the feasibility to converting constitutive promoters to PadR-controllable promoters. Moreover, four hybrid promoters without *yveF* and *yveG* inserted (P1, P2, P7, and P9) showed increased strength compared to P_{padC} and can be regulated by PadR and *p*-coumaric acid. In summary, the engineered PadR-P_{padC} biosensor system showed versatile dynamic performance or behaviors. These variants can be applied in dynamic regulation or high-throughput screening. Our work also provides valuable insights in how to optimize and engineer natural biosensor systems that are not suitable for immediate metabolic engineering application.

Results

Construction and Verification of PadR-P_{padC} biosensor system

According to the previously reported mechanism[15–17], the expression of PadR can repress P_{padC} promoter and inhibit the downstream gene *padC*. Upon induction of *p*-coumaric acid or ferulic acid, this repression can be released. This is a typical transcriptional factor-based biosensor system. To further understand and engineer the dynamic behavior of this biosensor system, we first constructed the functional biosensor system in *E. coli*. The *padR* gene was placed under the control of the constitutive promoter lpp1.0, and the reporter gene *egfp* was under the control of promoter P_{padC} cloned from *Bacillus subtilis* to create a regulator and a reporter plasmid, pCS-lpp1.0-PadR and pZE-P_{padC}-egfp, respectively (Fig. 2a). To validate the successful construction and regulation of the biosensor system, the previously reported PadR effector, *p*-coumaric acid, was utilized for induction. The strain containing only the reporter plasmid pZE-P_{padC}-egfp was used as a positive control (PC1, with no effector added). The fluorescence intensity normalized with OD_{600} (RFU/OD_{600}) was used to reflect the promoter activity of P_{padC}. As shown in Fig. 2b, the promoter activity of the uninhibited P_{padC} in positive control (PC1) was 2619.5 a.u.. The P_{padC} can work well without PadR inhibition. In the existence of pCS-lpp1.0-PadR (blank 1, with no inducer added), the fluorescence intensity was reduced to 44.5 a.u., indicating that 98.3% of the P_{padC} activity was repressed by PadR. After the addition of 600 mg/L *p*-coumaric acid, the fluorescence intensity was increased to 79.4 a.u. (Fig 2b). The results demonstrated that the *p*-coumaric

Author Manuscript Author Manuscript Author Manuscript Author Manuscript

acid successfully activated the biosensor system, which were consistent with previous studies[16], but the activated strength was too low to be applied in dynamic regulation or high-throughput screening compared with the commonly used biosensors. Proceeding further, we hypothesized that a better performance of this biosensor might be achieved by using different inducers. Thus, ferulic acid and the cinnamic acid with a similar structure to *p*-coumaric acid were used to induce the biosensor system. After the addition of 600 mg/L ferulic acid, the florescence intensity was only 72.8 a.u., which was even lower than the activated strength by *p*-coumaric acid. The addition of cinnamic acid did not result in any increase expression of *egfp* , indicating that this compound was unable to activate the biosensor (Fig 2b). To better illustrate the inducibility of different inducers, we tested the promoter performance under different concentrations of each inducer, as shown in Fig. 2e. With the increased concentration of *p*-coumaric acid and ferulic acid, the activated strength of P_{padC} increased, which further indicated that these two inducers can release the PadR repression. However, with the increase of cinnamic acid concentration, there was no increase in the *egfp* expression level (Fig. 2e), which proved that cinnamic acid cannot release the PadR repression. Taken together, there are some issues in the PadR-P_{padC} biosensor system, especially the limited dynamic range.

The poor performance of the biosensor system was presumably caused by high-level expression of PadR, as demonstrated in a previous study[17]. To optimize the biosensor system for further application, a series of lpp promoters (lpp0.8, lpp0.5, and lpp0.2) with gradually descending strength were used to fine-tune the PadR expression level[19], resulting in three additional regulator plasmids pCS-lpp0.8-PadR, pCS-lpp0.5-PadR, and pCS-lpp0.2-PadR (Fig. 2d). These were each co-transferred with the reporter plasmid pZE-P_{padC}-egfp to *E. coli* BW25113 (F'). The *p*-coumaric acid and ferulic acid were used as inducers. When PadR was expressed under the control of lpp0.8 and lpp0.5 (the promoter strength was 80% and 50% compared with lpp1.0, respectively) and fed with 600 mg/L *p*-coumaric acid or ferulic acid, the resumed activities were nearly the same as when PadR was controlled by lpp1.0, indicating that the P_{padC} was still tightly repressed by PadR (Fig. 2d). The PadR expression level was too high under the control of lpp0.8 and lpp0.5. However, when PadR was expressed under the control of lpp0.2 at 20% strength of lpp1.0, the addition of 600 mg/L *p*-coumaric acid or ferulic acid resulted in increased strengths of P_{padC} to 208.4 a.u. or 182.0 a.u., respectively, which accounted for 7.96% or 6.95% of the fully induced P_{padC} activity. The resumed activity was approximately 1.6-fold higher than that when PadR was controlled by lpp1.0. The results demonstrated that the repression by PadR can be partially released by decreasing the PadR expression level to 20%. The decreased expression level of PadR showed a positive effect on releasing the repression, which was consistent with the previously reported results[17]. However, while the availability of PadR is a related parameter in tuning the dynamic range of this biosensor, the increase of dynamic range obtained by tuning the expression of PadR was limited as the induced P_{padC} only showed up to 8% of fully induced promoter activity (PC1) when induced by 600 mg/L *p*-coumaric acid or ferulic acid. The lower activated strength will limit the applicability of this biosensor system in metabolic engineering. To further enhance the dynamic behavior of this biosensor, we sought to investigate whether the genetic components behind P_{padC} affect the dynamic behavior of the biosensor system.

Author Manuscript Author Manuscript Author Manuscript Author Manuscript

The downstream *yveF* and *yveG* of P_{padC} affects the dynamic performance of PadR-P_{padC}

There are two hypothetical genes, *yveF* and *yveG*, located in the intergenic region between the promoter P_{padC} and *padC* gene in *Bacillus subtilis* genome. However, the specific functions of these two genes in the regulation of the PadR-P_{padC} biosensor system have not been characterized thus far. We hypothesized that these two genes may affect the P_{padC} activity and the dynamic behavior of the system. To test this hypothesis, *yveF* and/or *yveG* were inserted between the promoter P_{padC} and the *egfp* gene to form three additional reporter plasmids: pZE-P_{padC}-yveF-egfp, pZE-P_{padC}-yveG-egfp, and pZE-P_{padC}-yveF-yveG-egfp (Fig. 3a).

To characterize whether the addition of these two genes will alter the promoter activity and lead to different expression levels of *egfp*, four reporter plasmids, pZE-P_{padC}-egfp, pZE-P_{padC}-yveF-egfp, pZE-P_{padC}-yveG-egfp, and pZE-P_{padC}-yveF-yveG-egfp were introduced into *E. coli* BW25113 (F') individually to determine the promoter activities. The highest promoter strength was observed when both *yveF* and *yveG* were presented (PC4), resulting in a normalized fluorescence intensity of 4855.4 a.u. (Fig. 3b), which is 85.3% higher than the activity of P_{padC}. As for promoters with either *yveF* (PC2) or *yveG* (PC3), the promoter activities only accounted for 2.3% or 40.2% of PC1, respectively (Fig. 3b). *YveF* and *yveG* may have a positive effect in increasing the output strength of P_{padC}. Next, we explored the influence of *yveF* and *yveG* on the regulation of this biosensor system. The aforementioned reporter plasmids were each co-transformed with the regulator plasmid pCS-lpp0.2-PadR into *E. coli* BW255113 (F'). When no inducer was present, all four promoters can be effectively repressed by PadR (Fig. 3c). When induced with 600 mg/L *p*-coumaric acid, these promoters showed varied activity. The highest fluorescence level was achieved by the promoter P_{padC}-yveF-yveG (P_{padC}-FG) with a normalized RFU/OD_{600} of 812.4 a.u., releasing 16.7% of the P_{padC}-FG activity (Fig. 3c). However, the promoter activities of the other three promoters induced by *p*-coumaric acid were relatively low. The promoter strength of P_{padC} and P_{padC}-yveG were 136.1 a.u. and 223.8 a.u., respectively. P_{padC}-yveF could not be activated by *p*-coumaric acid (Fig. 3c). The results demonstrated that in the existence of both *yveF* and *yveG*, the PadR repression can be better released. Similar patterns were observed when the regulator plasmids pCS-lpp0.5-PadR and pCS-lpp0.8-PadR were used to test the function of *yveF* and yveG (Fig. 3d&e). Therefore, the promoter P_{padC}-FG was used for our following experiments.

Taken together, the results indicated that only when both *yveF* and *yveG* were inserted between the P_{padC} and the *egfp*, the output strength will be increased. In the existence of *yveF* behind P_{padC} (PC2), it lost almost all the activity. However, when *yveG* was added behind P_{padC} (PC3), the promoter activity was a little bit higher than PC2. It is possible that between *yveG* and downstream gene *padC*, there is a weaker RBS which was responsible for the expression of *egfp*. When only adding *yveF*, the *egfp* cannot be expressed because of the lack of a functional RBS, and no output strength can be detected. When *yveF* and *yveG* were both added, it is possible that there is a weaker RBS which was responsible for the expression of *egfp*. An alternative possibility is that the successful expression of *yveF* and *yveG* may have a synergistic effect on increasing the promoter strength. Some other

Author Manuscript Author Manuscript Author Manuscript Author Manuscript

experiments were needed to verify whether *yveF* and *yveG* work as encoding proteins or nucleotide sequence (e.g., 5'-UTR) in the P_{padC}-PadR sensor system.

To further investigate the function of *yveF* and *yveG*, we expressed two genes in a separate operon under the control of lpp1.0 in a high-copy plasmid pSC. We introduced the regulator plasmid pCS-lpp0.2-PadR with the pZE-PpadC-egfp and pSC-lpp1.0-yveF-yveG. The leaking expression of P_{padC} increased when *yveF* and *yveG* were expressed in another plasmid compared to P_{padC} and P_{padC}-FG. After adding 600 mg/L p-coumaric acid, the induced activity of P_{padC}&FG was similarly to P_{padC}-FG, which was higher than the control P_{padC} (Fig. 3f). Therefore, even the *yveF* and *yveG* were expressed from a separate plasmid, it still enhanced the dynamic range of the PadR-P_{padC} system, which indicated that *yveF* and *yveG* may work as encoding proteins to assist relieving the inhibition of PadR. We noticed that when no PadR was introduced, the strain only exhibited a very low level of fluorescence. This was likely because the high expression of egfp caused significant burden on the cells, as the growth of this strain was notably slower than others.

PadR engineering to decrease the binding affinity with P_{padC}

Although the addition of *yveF* and *yveG* enhanced the activation efficiency of PadR-P_{padC} biosensor, the activity of P_{padC} induced by 600 mg/L *p*-coumaric acid was still less than 20% of the unrepressed promoter. We hypothesized that this was due to the tight binding between PadR and the P_{padC}. To test this hypothesis, we engineered the key binding residues of PadR to diminish the binding affinity between PadR and P_{padC}. The crystal structure of PadR was resolved by Yoon *et al*[18]. They characterized the key binding residues (K37, H38, S39, Q40, Q61, K64) between PadR and P_{padC}, and found that the mutation of these residues can decrease the binding affinity between PadR and the synthetic dsDNA[18]. To explore how the mutation of these residues affect the dynamic performance of PadR-P_{padC} biosensor system, the key residues were mutated to alanine. Alanine is a chiral amino acid with the shortest side chain, which has the potential to decrease the binding affinity effectively. Six mutants (K37A, H38A, S39A, Q40A, Q61A, K64A) were obtained. These PadR mutants were under the control of lpp0.2 promoter and were each co-transformed with pZE-P_{padC}-yveF-yveG-egfp to determine the dynamic performance. Although all the PadR mutants can inhibit the activity of P_{padC}-FG, there were five mutants (K37A, H38A, S39A, Q40A, Q61A) exhibiting the increased leaking expression (Fig. 4a). Especially, when P_{padC}-FG was repressed by pCS-lpp0.2-H38A, the leaking expression level can account for 14% of the unrepressed promoter activity (Fig. 4a). The potential reason that H38A showed the weakest binding affinity among all the mutants. When P_{padC}-FG was repressed by pCS-lpp0.2-K64A, only 0.12% leaking activity was observed. This was more stringent than the wild type PadR (Fig. 4a). This result is interesting as K64 was mutated to a smaller residue, but mutation has not caused increased leaking expression compared to wild type.

After adding 600 mg/L *p*-coumaric acid, there were four PadR mutants, H38A, S39A, Q40A, and K64A, showing increased activated strength compared with the wild type, especially the PadR mutants H38A. 68.3% of the P_{padC}-FG activity can be recovered by 600 mg/L *p*-coumaric acid (Fig. 4a). Another interesting mutant is the K64A, which was not only more stringent but also showed an elevated activity compared with wild-type PadR

Author Manuscript Author Manuscript Author Manuscript Author Manuscript

after induction. On the other hand, two mutants, K37A and Q61A, exhibited lowered induction activities compared with wild type (Fig. 4a). Taken together, we obtained two PadR mutants, K64A and H38A, which exhibited the increased inhibition efficiency and activated strength, respectively, compared with wild type PadR.

To better characterize the dynamic behavior of these two mutants (H38A and K64A), the dynamic range of wild type PadR, H38A, and K64A was measured with *p*-coumaric acid. As shown in Fig. 4b, different concentrations (from 0 to 1000 mg/L) of *p*-coumaric acid were used to induce the biosensor system. In the group of wild type PadR, the activated strength of the promoter increases as the *p*-coumaric acid concentration increases from 0 to 600 mg/L, with the highest activated strength of 859.0 a. u. in 600 mg/L. There was no obvious increasing in the promoter strength when concentration of *p*-coumaric acid is higher than 600 mg/L. Thus, the operational range of wild type PadR was from 0 to 600 mg/L and its dynamic range is from 68.4 a.u. to 859.0 a.u.. The variant K64A enabled a broader dynamic range and higher activated strength of the sensor system compared with the wild type PadR. The activated strength of the promoter P_{padC}-yveF-yveG combined with PadR (K64A) increased from 65.9 to 1083.7 a.u. with *p*-coumaric acid concentration increasing from 0 to 1000 mg/L. Therefore, this mutant is more suitable for high-throughput screening due to the expanded dynamic range. As for the variant H38A, the highest activated strength can be achieved at 200 mg/L *p*-coumaric acid. Although the responsive range of PadR (H38A) is narrower (0–200 mg/L) than the wild type PadR (0–600 mg/L), it can be activated with only 5 mg/L *p*-coumaric acid with the strength reaching to 916.4 a.u.. These results indicated that when equipped with the PadR (H38A), the sensor system became extremely sensitive and exhibited a higher strength. This variant may be suitable for dynamic regulation of the synthesis of *p*-coumaric acid or its derivatives. In summary, we obtained two PadR mutants H38A and K64A with broader dynamic ranges, increased sensitivity and activated strengths. The applicability of the PadR-P_{padC} biosensor system in metabolic engineering can be largely expanded by using these variants.

Understanding the molecular mechanism of PadR mutants by modeling structure analysis

To better understand the molecular mechanisms and why these PadR mutants displayed the different performance, the 3D structures of each PadR mutants were necessary. Yoon *et al* resolved the complex of PadR and the related nucleotide binding sequence in P_{padC}[18]. The crystal structure of PadR and related DNA sequence was obtained from PDB database (PDB ID: 5X11) , as shown in Fig.5a. The 3D structures of six PadR mutants were simulated in Pymol. After the structure analysis, we found that, in the wild type PadR, there are two hydrogen bonds between His38 and DNA sequence. However, the mutation in His38 eliminated the interaction between PadR and P_{padC} based on the simulation result (Fig. 5b&5c). The weaken interaction between H38A and DNA sequence might explain the leaking expression when depressing the P_{padC}. Besides, *p*-coumaric acid can better release the inhibition than wild type PadR possibly due to the decreased interaction, which also caused a higher activated strength. As for K64A, there is one hydrogen bond between Lys64 and DNA sequence in wild type PadR. According to the simulation result, though the hydrogen bond still existed after the mutation to Ala, the loop became more flexible than before, which might be favorable to combine with the DNA sequence (Fig. 5d & 5e). The

Author Manuscript Author Manuscript Author Manuscript Author Manuscript

better binding pattern was likely the reason for the increased inhibition efficiency of K64A compared to wild type PadR, and possibly the increased flexibility made the promoter more easily activated by *p*-coumaric acid. There are four mutants, K37A, S39A, Q40A, and Q61A, which exhibited the increased leaking expression compared to wild type PadR. The simulated structure analysis showed there were one hydrogen bond between residues Ser39, Gln40, Gln61 and their related DNA sequence (Fig. 6). However, after the mutation, this hydrogen bond was eliminated, and this possibly resulted in the decreased binding affinities. Because the Lys37 is positively charged, it can interact with the negatively charged bases, allowing PadR to bind closely to the P_{padC} (Fig. 6). When Lys37 was mutated to Ala, the electrostatic interaction disappeared and the binding capacity became weaker, which might be the reason for the increased leaking expression of K37A.

Constructing hybrid promoters to explore the “plug-and-play” possibility of PadR binding regions and increase the output strength of the biosensor system

There are two binding boxes, PadR-1 and PadR-2 located in the promoter P_{padC}[15] We hypothesized that the PadR binding regions can function in a “plug-and-play” manner, and thus placing these binding boxes in a constitutive promoter would convert it to a PadR-regulatable promoter. Besides, although P_{padC}-FG exhibited a higher strength compared to P_{padC} (Fig. 3), the strength was still relatively low compared with other biosensors used in metabolic engineering. Therefore, to investigate our hypothesis and further increase the output strength of the sensor system, we chose the strong constitutive promoter PL from phage lambda as a proof-of-concept demonstration to construct hybrid promoters. We hypothesized that by placing the PadR-1 and PadR-2 in the PL promoter, the newly constructed hybrid promoters can be regulated by *p*-coumaric acid and PadR, and they may also exhibit increased strength compared to wild type P_{padC}-FG.

The widely used constitutive promoter PL has been engineered to form different inducible promoters, such as PL_{lacO1}, PL_{tetO1}, and PL_{ara}. These inducible promoters were constructed by replacing the upstream 19 bp sequence before −35 region (Position 1) and 17 bp sequence between −35 region and −10 region (Position 2) with corresponding binding sequence (e.g LacO box and tetO box)[20]. Based on this design principle, we constructed eight hybrid promoters by placing PadR-1 (22 bp) and PadR-2 (22 bp) in Position 1 and Position 2, as shown in Fig. 7a. Because of the previously demonstrated positive effect of *yveF* and *yveG* on the performance of P_{padC}, the two genes were added behind all these eight hybrid promoters as well as the original PL promoter. We first determined the promoter activity of these eight hybrid promoters. Six hybrid promoters (P1-FG, P2-FG, P5-FG, P6-FG, P7-FG, and P8-FG) only accounted for less than 5% activity of the P_{padC}-FG (Fig. 7b). There were two hybrid promoters, P3 and P4, showed usable activities. We further verified whether the P3 and P4 can be regulated by the PadR and *p*-coumaric acid. When PadR was present, about 90% of the activities of P3 and P4 can be repressed (Fig. 7b). After adding 600 mg/L *p*-coumaric acid, about 30% and 68% of the activity can be activated for P3 and P4, respectively (Fig. 7b). On the contrary, the wild-type PL promoter cannot be regulated by PadR and activated by *p*-coumaric acid. Although there was a slight decrease in fluorescence level of PL promoter when PadR was introduced, this was likely due to the burden caused by the overexpression of PadR. The hybrid promoters P3 or P4 can be

Author Manuscript Author Manuscript Author Manuscript Author Manuscript

regulated by *p*-coumaric acid and PadR, but the promoter strengths were much lower compared with the P_{padC}-FG. We suspected that the insertion of *yveF* and *yveG* affected the transcription or translation of *egfp* when it was expressed under the control of hybrid promoters. The promoter structures or transcriptional machineries between P_{padC} and hybrid promoters may be different. Therefore, the existence of *yveF* and *yveG* may pose a detrimental effect on *egfp* expression because they were co-translated with this reporter gene, even though *yveF* and *yveG* have a positive effect on increasing P_{padC} strength in our previous experiment (Fig 3).

To test this hypothesis, we removed the *yveF* and *yveG* in the eight hybrid promoters. The promoter activities of these new hybrid promoters were determined. There are three hybrid promoters (P3, P5, and P6) which exhibited the decreased strength compared to wild type P_{padC}, although they can be regulated by PadR and *p*-coumaric acid. Another five promoters (P1, P2, P4, P7, P8) have increased strength compared to P_{padC}. In particular, the strength of P1, P2, and P7 increased by 119%, 109%, and 32% compared to P_{padC}-FG, respectively (Fig. 8b). The results confirmed our hypothesis. The potential reason was that the existence of *yveF* and *yveG* affected the expression of *egfp* because the three genes were co-expressed by one promoter, and the transcriptional machineries between P_{padC} and hybrid promoters may be very different. When PadR was introduced, more than 92% of the strength of P1, P2, P7, P8 can be repressed except P4, which cannot be repressed when PadR was introduced. After adding 600 mg/L *p*-coumaric acid, 37%, 26%, and 36% of the activity of P1, P2, and P7 can be obtained. The P8 cannot be induced by *p*-coumaric acid. This was likely due to stringent bind between PadR and the P8. Taken together, without the insertion of *yveF* and *yveG*, we obtained three hybrid promoters which not only can be regulated by PadR and *p*-coumaric acid but also have increased strength. The results also indicated that these two genes may pose detrimental effects on the *egfp* expression when they were placed after the hybrid promoters, even their expression can increase the strength of wild type P_{padC}.

We sought to construct a second series of hybrid promoters based on the position of two PadR binding sequences in P_{padC}. We constructed five hybrid promoters by placing the PadR binding sequences in the same position in PL as where they are in the P_{padC} promoter. For example, the PadR-1 starts from the +2 position in P_{padC} and ends in +23, and the sequence starting from the +2 position in PL will be replaced with PadR-1. Similarly, PadR-2, which is located from −13 to +9, can be placed in the corresponding location in PL. All the hybrid promoters using this design have two groups, one group was with *yveF* an *yveG* behind the promoters and the other one was without the insertion of these two genes. The design principles for the five hybrid promoters in the first group was shown in Fig. 7a. All the five promoters only accounted for less than 40% activity of the P_{padC}-FG. The potential reason was likely the same as what in the first round of hybrid promoters that the existence of *yveF* and *yveG* behind the hybrid promoters negatively affected the expression of *egfp* (Fig. 7c). Therefore, the *yveF* and *yveG* were removed in the hybrid promoters. After the elimination of *yveF* and *yveG*, there were two promoters, P9 and P11, exhibiting 147% and 112% strength increase compared to P_{padC}-FG. Another three promoters, P10, P12, and P13 have decreased strength compared to P_{padC}-FG. When co-transferred with pCS-lpp0.2-PadR, 96% of P9's activity can be repressed and 50% of the activity can be obtained after adding 600 mg/L *p*-coumaric acid. As for P11, it cannot be activated by 600 mg/L *p*-coumaric acid

Author Manuscript Author Manuscript Author Manuscript Author Manuscript

though it can be repressed by PadR (Fig. 8c). We also noticed that the positive control of P12 without PadR cannot grow well, which led to very low fluorescence level. These results indicated that the constitutive promoter can be engineered to be regulated by PadR and *p*-coumaric acid.

So far, four hybrid promoters (P1, P2, P7, and P9) without *yveF* and *yveG* insertion exhibited an increased strength compared to P_{padC}-FG, which showed the best performance among the wild-type promoters. Because of the positive effect of *yveF* and *yveG* in PadR-P_{padC} biosensor system, we further explored the performance of the best four hybrid promoters (P1, P2, P7, and P9) with the existence of pSC-lpp1.0-yveF-yveG. The results indicated that the maximum promoter strength of P1&FG, P2&FG, P7&FG, and P9&FG exhibited 30%, 42%, 24%, and 22% decrease compared to the promoter strength of P1, P2, P7, and P9, respectively. The potential reason was that co-transferring two plasmids caused the burden on cells which might decrease the *egfp* expression. When PadR was introduced, four hybrid promoters (P1&FG, P2&FG, P7&FG, and P9&FG) can be repressed by PadR with higher leaking activities except P1&FG. When 600 mg/L *p*-coumaric acid was added, the activity of four hybrid promoters can be obtained with higher strength compared to the promoters without the *yveF* and *yveG* overexpression (Fig. 9). These results further confirmed that *yveF* and *yve*G can function as proteins and positively assist the inhibition release.

Conclusion

Transcriptional factor-based biosensors played a significant role in metabolic engineering. They can be utilized to dynamically regulate the pathway for the synthesis of valuable compounds or used for high-throughput screening of high yield strains. In this paper, we cloned and optimized the *p*-coumaric acid responsive regulator PadR from *Bacillus subtilis.* After functional analysis and verification, we found that *yveF* and *yveG* showed a significant impact on the regulation of PadR-P_{padC} biosensor system, mostly on increasing the P_{padC} strength and assisting the repression release. In the existence of *yveF* and *yveG*, the promoter strength of P_{padC}-FG increased 80% compared with P_{padC}. In addition, when *p*-coumaric acid added, the activated efficiency increased 116%. To further increase the dynamic range of PadR-P_{padC} biosensor system, we designed six PadR mutants and obtained two mutants with increased dynamic range and sensitivity. The mutant K64A exhibited a broader operational range (0–1000 mg/L) compared to wild type PadR (0–600 mg/L). The highest activated strength reached 1083.7 a.u., which is 1.26-fold higher than wild type PadR. The other mutant H38A, which achieved the highest activated strength at 200 mg/L *p*-coumaric acid, was extremely sensitive and it can be activated with even only 5 mg/L *p*-coumaric acid. We also revealed the molecular mechanism of how these mutants affected the dynamic behavior of this biosensor system based on rational structure analysis of PadR. Finally, a series of hybrid promoters, which were engineered to be regulated by PadR and *p*-coumaric acid, were constructed. Four of them P1, P2, P7, and P9 showed increased strength compared to P_{padC} and can be regulated by PadR and *p*-coumaric acid. The PadR and P_{padC} variants we obtained in this paper expanded the application of this biosensor system in dynamic regulation and high-throughput screening.

Author Manuscript Author Manuscript Author Manuscript Author Manuscript

Materials and methods

Strains, plasmids, and hybrid promoter sequence

High-copy number plasmid pZE12-luc and medium-copy number plasmid pCS27 were used for plasmids construction. *E. coli* strains XL1-Blue and BW25113 (F') were used for plasmids construction and biosensor characterization, respectively. Strains and plasmids used in this paper were shown in Table 1. *Bacillus subtilis* was used for *PadR*, *yveF*, *yveG*, and P_{padC} clone.

Spacer sequence before *yveF:*

GAGGTGGTTCTC

Spacer sequence between *yveF and yveG:*

TTCATTCCGATTCGTTCGGGAACAATAACCGGGGAAGTAAAGGGACGTATTTTGC CGGGCGGTGCCGATTCACAA

Spacer sequence between *yveG* and downstream *padC*

AAGACTAAGGAGAGTGTGTAAG

Hybrid promoters with *yveF* and *yveG* were constructed by adding two genes behind related hybrid promoters directly.

Medium and chemicals

For plasmids construction and biosensor characterization, Luria-Bertani (LB) medium containing 10 g/L NaCl, 5 g/L yeast extract, and 10 g/L tryptone was used in strains inoculation. The antibiotics ampicillin and kanamycin were added in the culture as needed with the final concentration of 100 μg/mL and 50 μg/mL, respectively. For the preparation of inducer solution, 100 mg *p*-coumaric acid, ferulic acid, cinnamic acid, and caffeic acid were dissolved into 1mL methanol, respectively. *p*-coumaric acid, ferulic acid, cinnamic acid, and caffeic acid were purchased from MP Biomedicals. Methanol was purchased from Fisher Chemicals. High-Fidelity Phusion DNA polymerase, restriction endonucleases, and Quick Ligation Kit were purchased from New England Biolabs (Beverly, MA, USA). Zyppy™ Plasmid Miniprep Kit, Zymoclean™ Gel DNA Recovery Kit, and DNA Clean & Concentrator™−5 were purchased from Zymo Research (Irvine, CA, USA).

DNA manipulation

PadR, *yveF*, *yveG*, and P_{padC} were amplified from genome DNA of *Bacillus subtilis*. P_{padC} digested by XhoI and KpnI was cloned into pCS-lpp1.0-*egfp* to construct the plasmid pZE-P_{padC}-*egfp*. The same methods were used to construct plasmids pZE-P_{padC} -yveF-egfp, pZE-P_{padC} -yveF-yveG-egfp. P_{padC} and *yveG* were combined by overlap extension PCR to obtain the fragments P_{padC}-yveG. P_{padC}-yveG digested by XhoI and KpnI was cloned into pCS-lpp1.0-egfp to construct the plasmid pZE- P_{padC} -yveG-egfp. *PadR* digested by KpnI and BamHI was cloned into pCS-lpp1.0-egfp to construct the plasmid pCS-lpp1.0-PadR. Same methods in pCS-lpp1.0-PadR construction were used to construct the plasmids pCS-lpp 0.8-

Author Manuscript Author Manuscript Author Manuscript Author Manuscript

PadR, pCS-lpp 0.5-PadR, and pCS-lpp 0.2-PadR. YveF-yveG were digested by EcoRI and BamHI was cloned into pCS-lpp1.0-egfp to construct the plasmid pCS-lpp1.0-egfp. pCS-lpp1.0-egfp was used as template to get the fragment of lpp1.0-yveF-yveG. lpp1.0-yveF-yveG digested by XhoI and BamHI was cloned to pSC-egfp to get the plasmid pSC-lpp1.0-yveF-yveG.

Mutants construction

Site-directed mutation of PadR was carried out by overlap extension PCR using plasmid pCS-lpp0.2-*PadR* as template. The primer containing PL was synthesized containing the restriction site of XhoI. The fragment PL-yveF-yveG-egfp digested by XhoI and XbaI was cloned into pZE-PLlacO1 to construct the plasmid pZE-PL-yveF-yveG-egfp, which was used as the template for hybrid promoter's construction. The hybrid promoter digested by AatII and EcoRI was cloned to pZE-egfp to get the hybrid promoters without *yveF* and *yveG*.

Dynamic range characterization of PadR-P_{padC} biosensor system

Specific plasmids were transformed into *E. coli* BW25113 (F'), respectively. After 12 hours, single colony was picked and inoculated into 3.5 mL LB medium containing specific antibiotics. After 10 hours of cultivation, the cultures were transferred into 15 mL test tubes containing 3.5 mL LB medium and specific antibiotics, with an inoculation ratio of 5%. When OD_{600} reached 0.4, different amounts of 100 g/L inducers were added to the specific concentration. After 12 hours, 100 μL cell culture were sampled for fluorescence assay. All experiments were carried out with three groups.

Fluorescence assay

Cell cultures (100 μL) were transferred into a black 96-well plate (BRAND plates) and diluted with equal volume of water. The fluorescence intensity of egfp was detected with Biotek Synergy HT plate reader using excitation filter of 520 nm, and emission filter of 485 nm. The egfp fluorescence intensity of each sample was normalized against its OD_{600} and background cell fluorescence was subtracted.

$$\frac{RFU}{OD_{600}} = \frac{fluorescence - 100}{(optical\ density\ at\ 600\,nm - 0.043) * 1.76}$$

ACKNOWLEDGMENTS

This work was supported by the National Institute of General Medical Sciences of the National Institutes of Health under award number R35GM128620. We also acknowledge the support from the College of Engineering, The University of Georgia, Athens

Reference

[1]. Zhou Y, Lin L, Wang H, Zhang Z, Zhou J, and Jiao N (2020) Development of a CRISPR/Cas9n-based tool for metabolic engineering of Pseudomonas putida for ferulic acid-to-polyhydroxyalkanoate bioconversion, Commun Biol 3, 98. [PubMed: 32139868]

[2]. Zhu M, Wang C, Sun W, Zhou A, Wang Y, Zhang G, Zhou X, Huo Y, and Li C (2018) Boosting 11-oxo-beta-amyrin and glycyrrhetinic acid synthesis in Saccharomyces cerevisiae via pairing

Author Manuscript Author Manuscript Author Manuscript Author Manuscript

novel oxidation and reduction system from legume plants, Metab Eng 45, 43–50. [PubMed: 29196123]

[3]. Florez AB, Alvarez S, Zabala D, Brana AF, Salas JA, and Mendez C (2015) Transcriptional regulation of mithramycin biosynthesis in Streptomyces argillaceus: dual role as activator and repressor of the PadR-like regulator MtrY, Microbiology 161, 272–284. [PubMed: 25416691]

[4]. Humphreys CM, and Minton NP (2018) Advances in metabolic engineering in the microbial production of fuels and chemicals from C1 gas, Curr Opin Biotechnol 50, 174–181. [PubMed: 29414057]

[5]. Wang J, Shen X, Yuan Q, and Yan Y (2018) Microbial synthesis of pyrogallol using genetically engineered Escherichia coli, Metab Eng 45, 134–141. [PubMed: 29247864]

[6]. Wang J, Zhang R, Zhang Y, Yang Y, Lin Y, and Yan Y (2019) Developing a pyruvate-driven metabolic scenario for growth-coupled microbial production, Metab Eng 55, 191–200. [PubMed: 31348998]

[7]. Yang Y, Lin Y, Wang J, Wu Y, Zhang R, Cheng M, Shen X, Wang J, Chen Z, Li C, Yuan Q, and Yan Y (2018) Sensor-regulator and RNAi based bifunctional dynamic control network for engineered microbial synthesis, Nat Commun 9, 3043. [PubMed: 30072730]

[8]. Xu P, Li L, Zhang F, Stephanopoulos G, and Koffas M (2014) Improving fatty acids production by engineering dynamic pathway regulation and metabolic control, Proc Natl Acad Sci U S A 111, 11299–11304. [PubMed: 25049420]

[9]. Gupta A, Reizman IM, Reisch CR, and Prather KL (2017) Dynamic regulation of metabolic flux in engineered bacteria using a pathway-independent quorum-sensing circuit, Nat Biotechnol 35, 273–279. [PubMed: 28191902]

[10]. Zhang F, Carothers JM, and Keasling JD (2012) Design of a dynamic sensor-regulator system for production of chemicals and fuels derived from fatty acids, Nat Biotechnol 30, 354–359. [PubMed: 22446695]

[11]. Lan EI, and Liao JC (2012) ATP drives direct photosynthetic production of 1-butanol in cyanobacteria, Proc Natl Acad Sci U S A 109, 6018–6023. [PubMed: 22474341]

[12]. Dietrich JA, Shis DL, Alikhani A, and Keasling JD (2013) Transcription factor-based screens and synthetic selections for microbial small-molecule biosynthesis, ACS Synth Biol 2, 47–58. [PubMed: 23656325]

[13]. Chen W, Zhang S, Jiang P, Yao J, He Y, Chen L, Gui X, Dong Z, and Tang SY (2015) Design of an ectoine-responsive AraC mutant and its application in metabolic engineering of ectoine biosynthesis, Metab Eng 30, 149–155. [PubMed: 26051748]

[14]. Xu P, Wang W, Li L, Bhan N, Zhang F, and Koffas MA (2014) Design and kinetic analysis of a hybrid promoter-regulator system for malonyl-CoA sensing in Escherichia coli, ACS Chem Biol 9, 451–458. [PubMed: 24191643]

[15]. Nguyen TK, Tran NP, and Cavin JF (2011) Genetic and biochemical analysis of PadR-padC promoter interactions during the phenolic acid stress response in Bacillus subtilis 168, J Bacteriol 193, 4180–4191. [PubMed: 21685295]

[16]. Tran NP, Gury J, Dartois V, Nguyen TK, Seraut H, Barthelmebs L, Gervais P, and Cavin JF (2008) Phenolic acid-mediated regulation of the padC gene, encoding the phenolic acid decarboxylase of Bacillus subtilis, J Bacteriol 190, 3213–3224. [PubMed: 18326577]

[17]. Siedler S, Khatri NK, Zsohar A, Kjaerbolling I, Vogt M, Hammar P, Nielsen CF, Marienhagen J, Sommer MOA, and Joensson HN (2017) Development of a Bacterial Biosensor for Rapid Screening of Yeast p-Coumaric Acid Production, ACS Synth Biol 6, 1860–1869. [PubMed: 28532147]

[18]. Park SC, Kwak YM, Song WS, Hong M, and Yoon SI (2017) Structural basis of effector and operator recognition by the phenolic acid-responsive transcriptional regulator PadR, Nucleic Acids Res 45, 13080–13093. [PubMed: 29136175]

[19]. Wang J, Mahajani M, Jackson SL, Yang Y, Chen M, Ferreira EM, Lin Y, and Yan Y (2017) Engineering a bacterial platform for total biosynthesis of caffeic acid derived phenethyl esters and amides, Metab Eng 44, 89–99. [PubMed: 28943460]

Author Manuscript Author Manuscript Author Manuscript Author Manuscript

[20]. Lutz R, and Bujard H. J. N. a. r. (1997) Independent and tight regulation of transcriptional units in Escherichia coli via the LacR/O, the TetR/O and AraC/I1-I2 regulatory elements, 25, 1203–1210.

[21]. Shen CR, and Liao JC (2008) Metabolic engineering of Escherichia coli for 1-butanol and 1-propanol production via the keto-acid pathways, Metab Eng 10, 312–320. [PubMed: 18775501]

Author Manuscript Author Manuscript Author Manuscript Author Manuscript

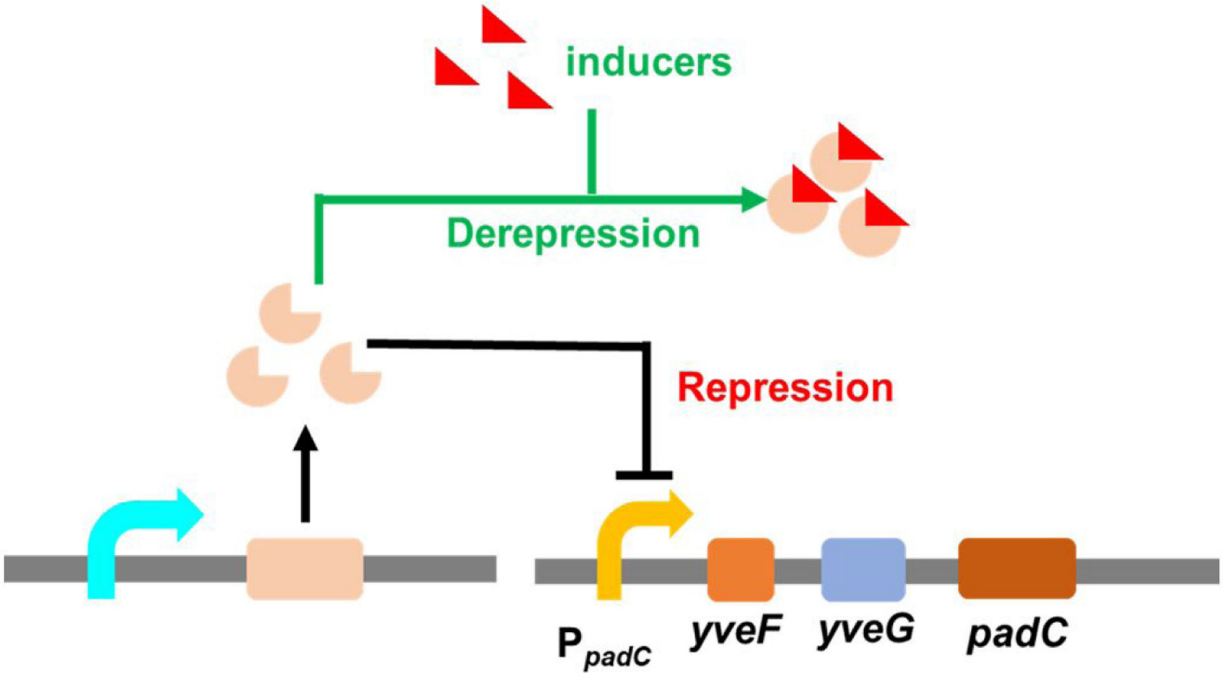

Fig. 1.

the mechanism of PadR-P_{padC} biosensor system. **Repression**: PadR binds in the specific regions in P_{padC}, which repressed the expression of *padC* gene. **Derepression:** In the existence of inducers, they can combine with PadR and released the inhibition of P_{padC}. *padC* gene can express.

Author Manuscript
Author Manuscript
Author Manuscript
Author Manuscript

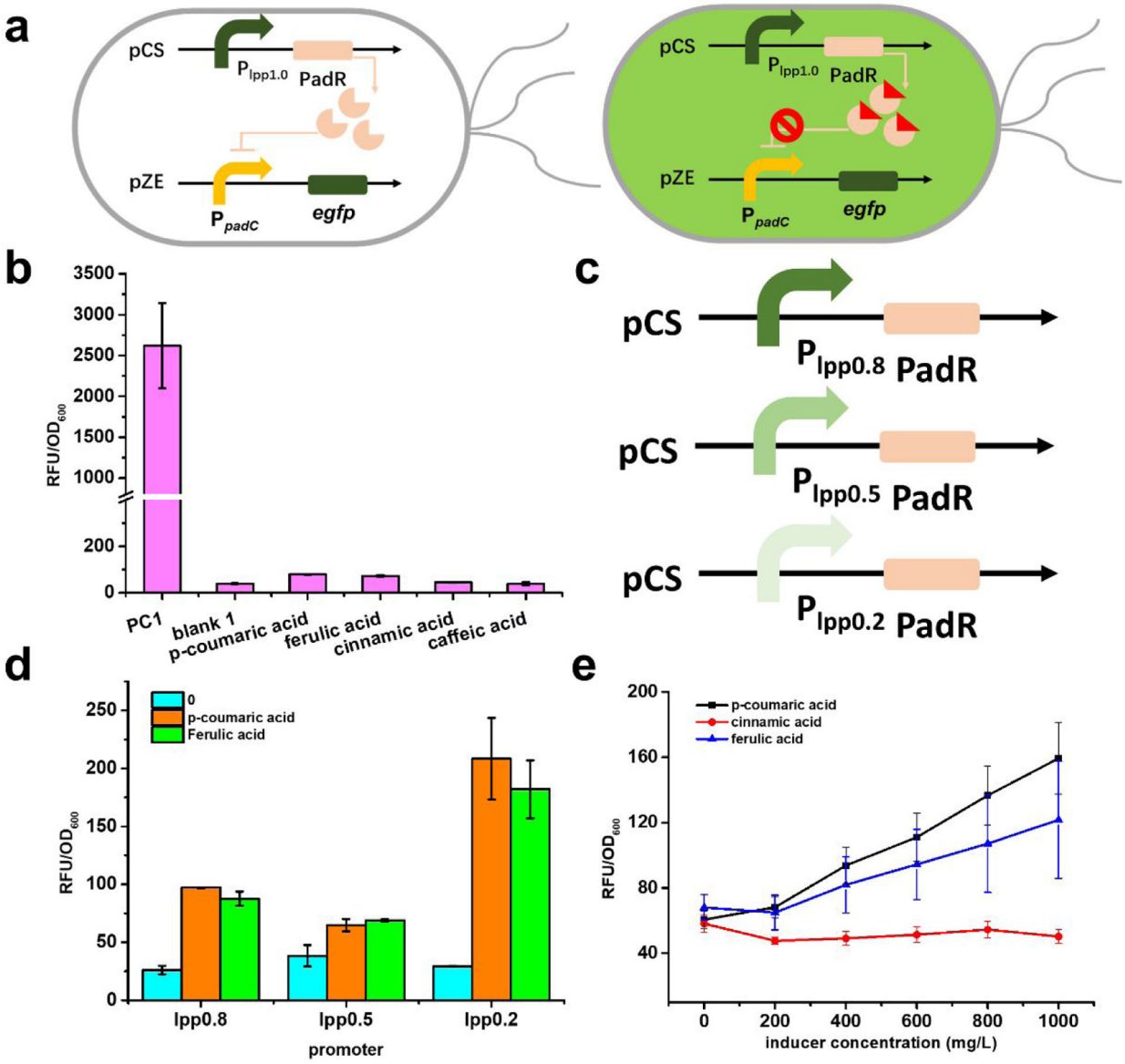

Fig. 2.

The design of PadR-P_{padC} biosensor system and its optimization. **(a)** The genetic circuit of PadR-P_{padC} biosensor system. There are two modules in this system, reporter module and regulator module. In the absence of *p*-coumaric acid, PadR can repress the P_{padC} and egfp cannot express successfully. When *p*-coumaric acid was added, it can bind to PadR, which released the inhibition of P_{padC}; the green fluorescence can be detected. **(b)** The promoter strength with or without PadR inhibition. PC1, without regulator module, was used to test the strength of P_{padC}; blank, with reporter module and regulator module, which was used to characterize the inhibition efficiency; *p*-coumaric acid, ferulic acid, and cinnamic acid represent that different inducers were added to release the PadR inhibition. **(c)** Different inducers in different concentration. P-coumaric acid, ferulic acid, and cinnamic acid were used as inducers to release the inhibition by pCS-lpp1.0-PadR. **(d)** Differe nt regulator modules with various promoter. **(e)** The effects of different expression level of PadR in

Author Manuscript Author Manuscript Author Manuscript Author Manuscript

decreasing its inhibition activity. All data are reported as mean±s.d. from three independent experiments (n=3). Error bars are defined as s.d.

Author Manuscript Author Manuscript Author Manuscript Author Manuscript

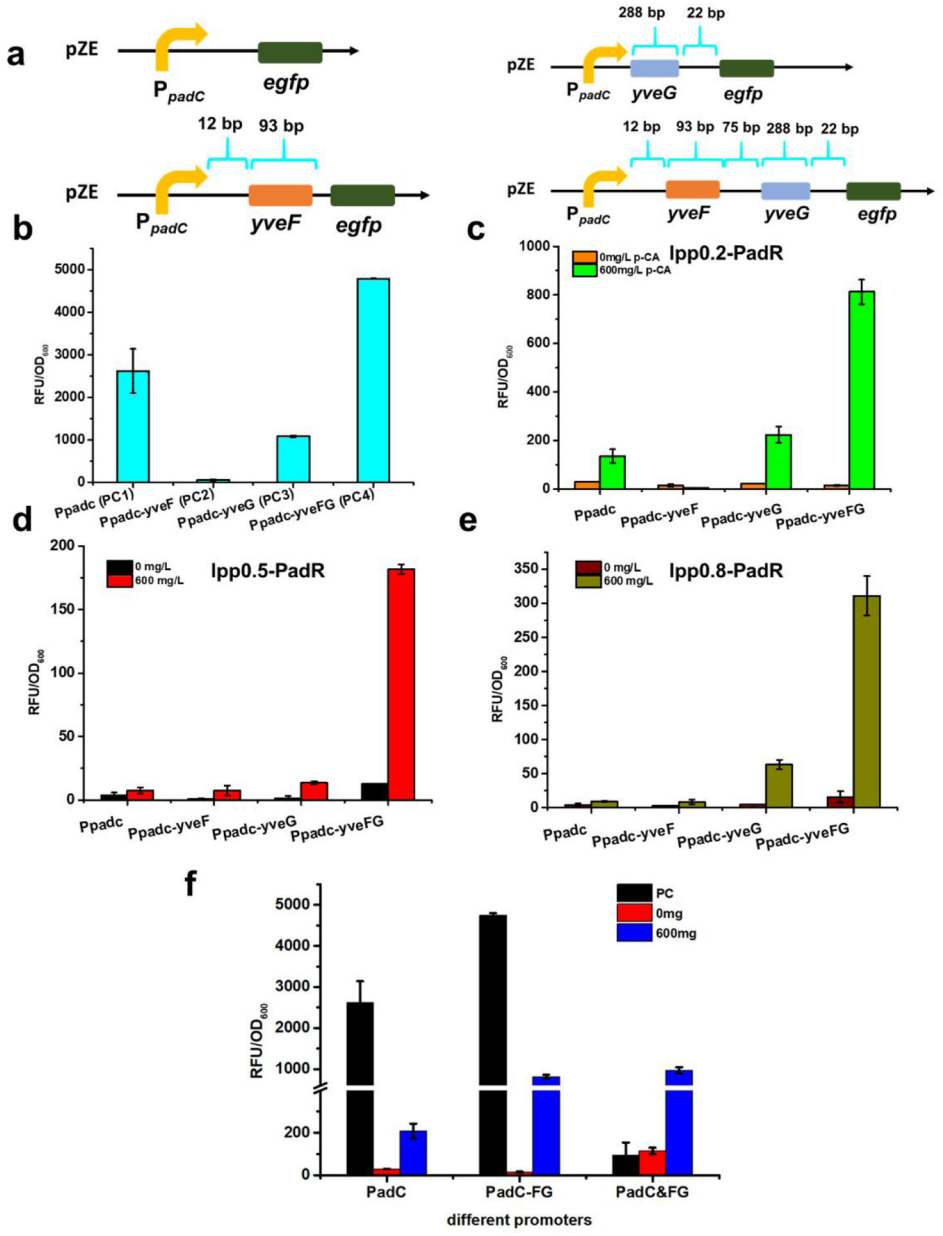

Fig. 3.

Exploring the function of *yveF* and *yveG* in the biosensor system. **(a)** Different reporter modules with or without *yveF* and yveG. *yveF*: 93 bp; *yveG*: 288 bp. Between *yveF* and *yveG*, there is a 75 bp spacer sequence. Between P_{padC}-yveF, there is a 12 bp spacer sequence. Between *yveG* and downstream *padC* gene, there is a 22 bp spacer sequence. To construct pZE-P_{padC}-yveF-egfp, the sequence of P_{padC}, *yveF*, and spacer sequence between P_{padC}-yveF were inserted before *egfp*. To construct pZE-P_{padC}-yveG-egfp, the sequence of P_{padC}, *yveG*, and the spacer sequence between *yveG* and downstream gene *padC* were inserted before *egfp*. To construct pZE-P_{padC}-yveF-yveG-egfp, the sequence of P_{padC}, spacer sequence between P_{padC} and *yveF*, *yveF*, the spacer sequence between *yveF* and *yveG*, *yveG*, and the spacer sequence between *yveG* and *padC* were inserted before egfp. **(b)** The

promoter strength without PadR inhibition. **(c)** The biosensor performance in the existence of pCS-lpp0.2-PadR and p-coumaric. **(d)** pCS-lpp0.5-PadR was used as the regulator plasmid. **(e)** pCS-lpp0.8-PadR was used as the regulator plasmid. **(f)** The biosensor performance with/without *yveF* and *yveG* before *egfp*, or when *yveF* and *yveG* were expressed independently. All data are reported as mean±s.d. from three independent experiments (n=3). Error bars are defined as s.d.

Author Manuscript Author Manuscript Author Manuscript Author Manuscript

Author Manuscript Author Manuscript Author Manuscript Author Manuscript

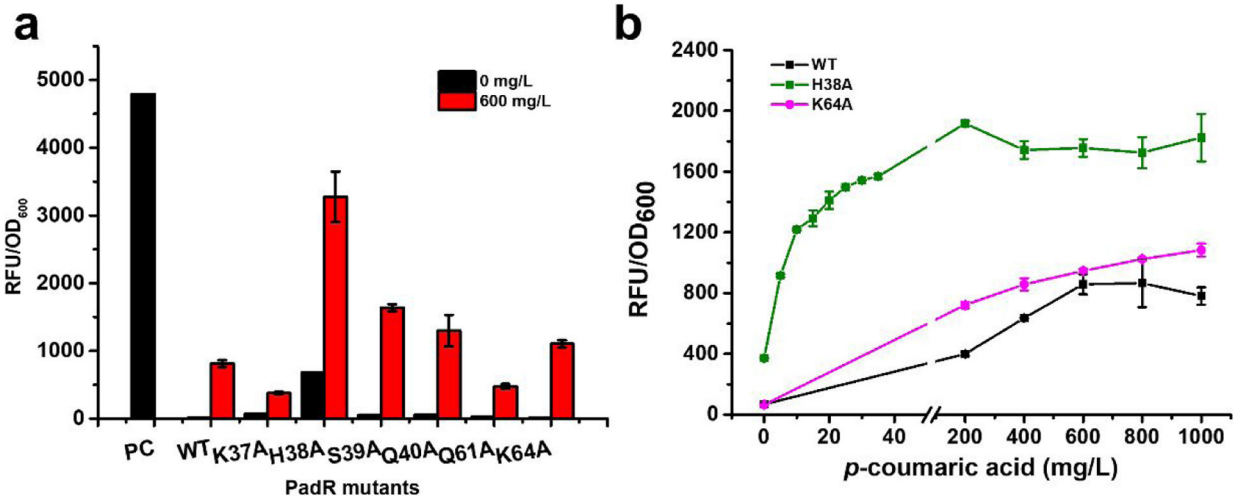

Fig. 4.

The dynamic behavior of different PadR mutants. **(a)** The different PadR mutants were tested by 0 and 600 mg/L *p*-coumaric acid; PC means the strain without regulator module. **(b)** The dynamic range of WT, H38A, K64A. All data are reported as mean±s.d. from three independent experiments (n=3). Error bars are defined as s.d.

Author Manuscript Author Manuscript Author Manuscript Author Manuscript

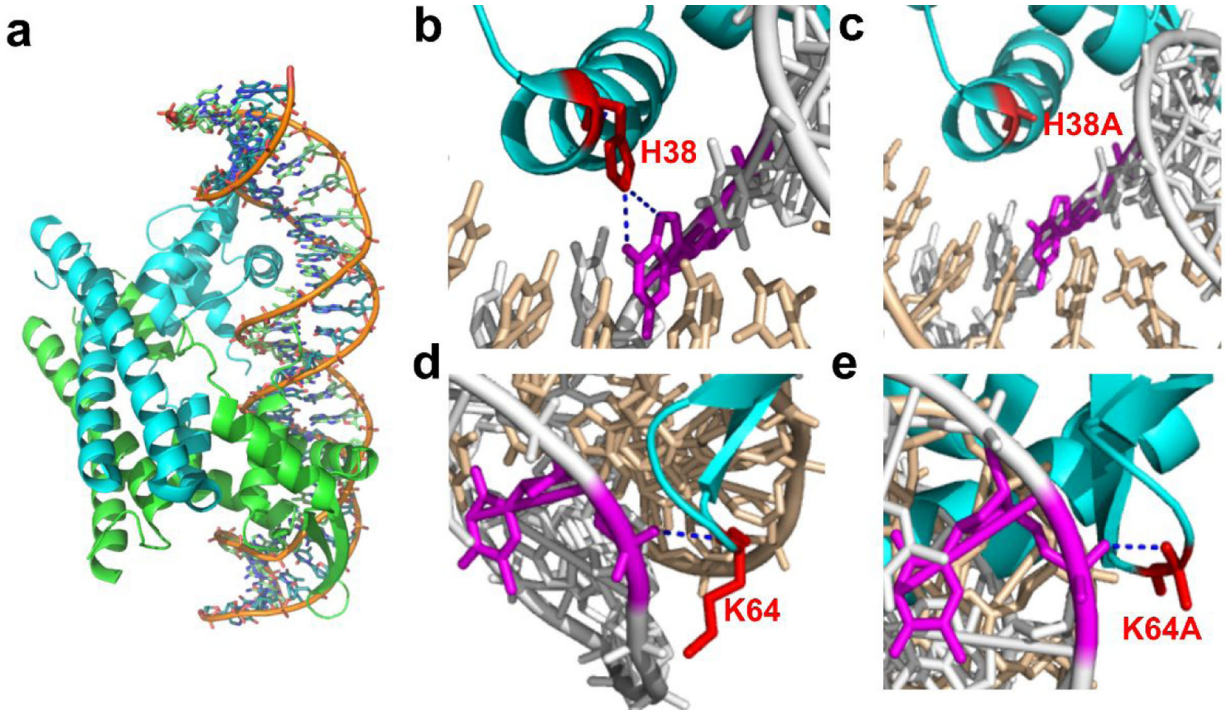

Fig. 5.

The structure analysis of PadR mutants. **(a)** The crystal structure of PadR and related DNA sequence. **(b)** The interaction between H38 and dsDNA. **(c)** The interaction between H38A and dsDNA. **(d)** The interaction between K64 and dsDNA. **(e)** The interaction between K64A and dsDNA.

Author Manuscript Author Manuscript Author Manuscript Author Manuscript

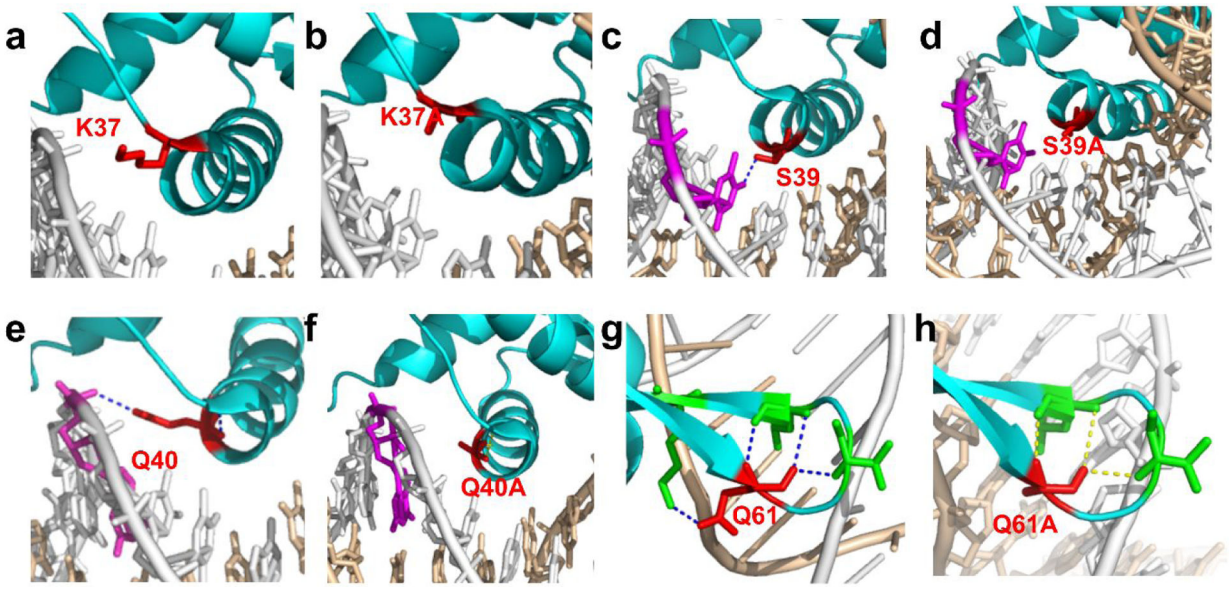

Fig. 6.

the modeling structure analysis of PadR mutants. **(a)** The interaction between K37 and dsDNA. **(b)** The interaction between K37A and dsDNA. **(c)** The interaction between S38 and dsDNA. **(d)** The interaction between S39A and dsDNA. **(e)** The interaction between Q40 and dsDNA. **(f)** The interaction between Q40A and dsDNA. **(g)** The interaction between Q61 and dsDNA. **(h)** The interaction between Q61A and dsDNA.

Author Manuscript Author Manuscript Author Manuscript Author Manuscript

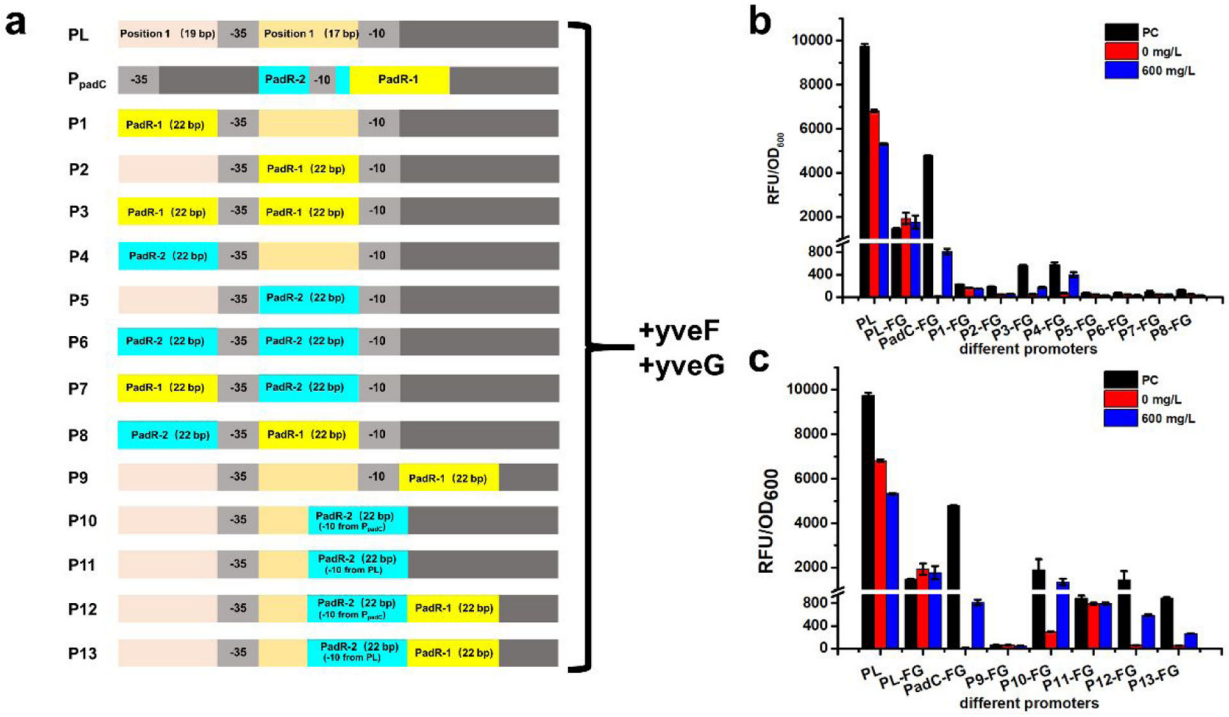

Fig. 7.

The performance of hybrid promoters with *yveF* and *yveG*. **(a)** The design of hybrid promoters. From P1-FG to P8-FG, PadR-1 and PadR-2 were placed before −35 region or −10 region simultaneously or respectively. The P9-FG and P10-FG contained only PadR-1 and PadR-2, respectively. Because the PadR-2 overlapped with the −10 region, and this may affect the promoter performance, we designed another hybrid promoter P11-FG by keeping the −10 sequence from PL. For hybrid promoters P12-FG and P13-FG, they contained both PadR binding boxes, but in P12-FG the −10 sequence from PpadC was used and in the P13-FG the −10 sequence from PL was used **(b)** The hybrid promoters designed according to PLlacO1 were rested by 0 and 600 mg/L *p*-coumaric acid. **(c)** The hybrid promoters, which were designed based on the relative position in P_{padC}, were tested by 0 and 600 mg/L *p*-coumaric acid. All data are reported as mean±s.d. from three independent experiments (n=3). Error bars are defined as s.d.

Author Manuscript Author Manuscript Author Manuscript Author Manuscript

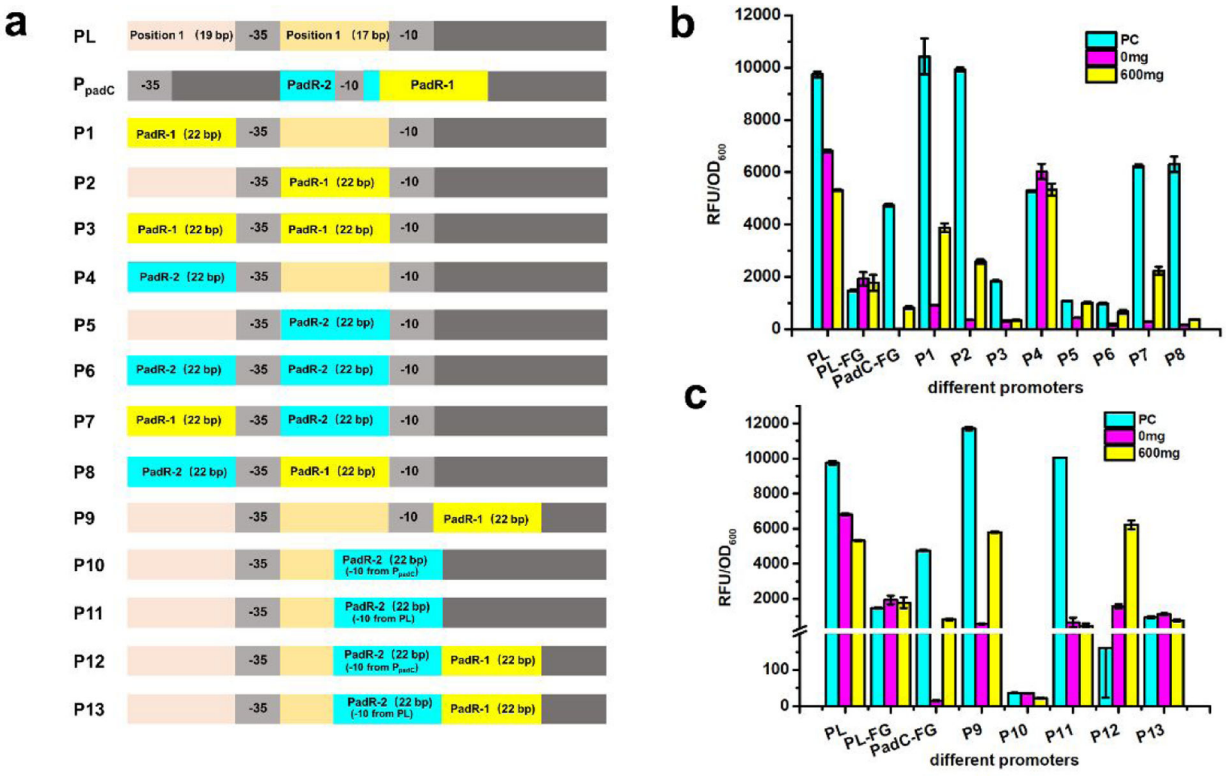

Fig. 8.

The performance of hybrid promoters without *yveF* and *yveG*. **(a)** The design of hybrid promoters. **(b)** The hybrid promoters designed according to PL_{lacO1} were rested by 0 and 600 mg/L *p*-coumaric acid. **(c)** The hybrid promoters, which were designed based on the relative position in P_{padC}, were tested by 0 and 600 mg/L *p*-coumaric acid. All data are reported as mean±s.d. from three independent experiments (n=3). Error bars are defined as s.d.

Author Manuscript Author Manuscript Author Manuscript Author Manuscript

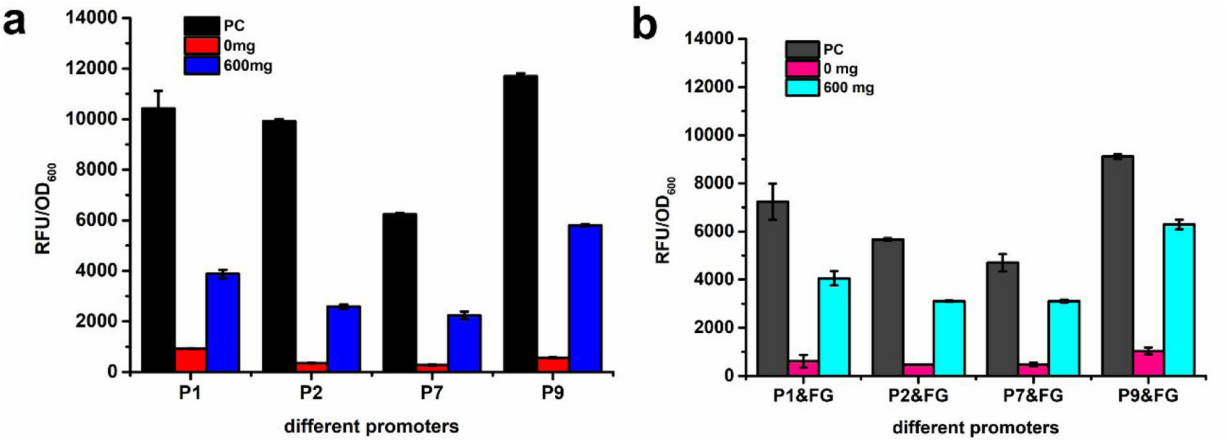

Fig. 9.

The dynamic performance of hybrid promoters without *yveF* and *yveG* or expressing *yveF* and *yveG* independently. (a) The dynamic performance of P1, P2, P7, and P9, which without *yveF* and *yveG*. (b) The dynamic performance of P1&FG, P2&FG, P7&FG, and P9&FG, which express *yveF* and *yveG* independently. All data are reported as mean±s.d. from three independent experiments (n=3). Error bars are defined as s.d.

Author Manuscript Author Manuscript Author Manuscript Author Manuscript

Table 1

List of strains and plasmids used in this study

Strains	Genotype	Reference
XL 1-Blue	*recA1 endA1gyrA96thi-1hsdR17supE44relA1lac [F' proAB lacIqZDM15n1O (TetR)]*	Stratagene
BW25113(F')	*rrnBT14 ΔlacZWJ16 hsdR514 ΔaraBADAH33 ΔrhaBADLD78 F' [traD36 proAB lacIqZΔM15 Tn10(Tetr)]*	Yale CGSC

Plasmids	Description	Reference
pZE12-luc	pLlacO-1; luc; *ColE1 ori; Amp^R*	20
pCS27	pLlacO-1; *p15A ori; Kan^R*	21
pZE-P$_{padC}$-*egfp*	pZE12-*luc* carrying P$_{padC}$ from *Bacillus subtilis* and *egfp*	In this study
pZE-P$_{padC}$-yveF-*egfp*	pZE12-*luc* carrying P$_{padC}$ and *yveF* from *Bacillus subtilis* and *egfp*	In this study
pZE-P$_{padc}$-yveG-*egfp*	pZE12-*luc* carrying P$_{padC}$ and *yveG* from *Bacillus subtilis* and *egfp*	In this study
pZE-P$_{padC}$-yveF-*yveG-egfp*	pZE12-*luc* carrying P$_{padC}$ and *yveF* and *yveG* from *Bacillus subtilis* and *egfp*	In this study
pCS-lpp1.0-*PadR*	pCS27 carrying promoter lpp1.O and *PadR* from *Bacillus subtilis*	In this study
pCS-lpp0.8-*PadR*	pCS27 carrying promoter lpp0.8 and *PadR* from *Bacillus subtilis*	In this study
pCS-lpp0.5-*PadR*	pCS27 carrying promoter lpp0.5 and *PadR* from *Bacillus subtilis*	In this study
pCS-lpp0.2-*PadR*	pCS27 carrying promoter lpp0.2 and *PadR* from *Bacillus subtilis*	In this study
pCS-lpp0.2-K37A	pCS27 carrying promoter lpp0.2 and *PadR* mutant K37A from *Bacillus subtilis*	In this study
pCS-lpp0.2-H38A	pCS27 carrying promoter lpp0.2 and *PadR* mutant H38A from *Bacillus subtilis*	In this study
pCS-lpp0.2-S39A	pCS27 carrying promoter lpp0.2 and *PadR* mutant S39A from *Bacillus subtilis*	In this study
pCS-lpp0.2-Q40A	pCS27 carrying promoter lpp0.2 and *PadR* mutant Q40A from *Bacillus subtilis*	In this study
pCS-lpp0.2-Q61A	pCS27 carrying promoter lpp0.2 and *PadR* mutant Q61A from *Bacillus subtilis*	In this study
pCS-lpp0.2-K64A	pCS27 carrying promoter lpp0.2 and *PadR* mutant K64A from *Bacillus subtilis*	In this study
pZE-P1-yveF-yveG-egfp	pZE12-*luc* carrying P$_{padC}$ mutant P1, and *yveF* and *yveG* from *Bacillus subtilis* and *egfp*	In this study
pZE-P2-yveF-yveG-egfp	pZE12-*luc* carrying P$_{padC}$ mutant P2, and *yveF* and *yveG* from *Bacillus subtilis* and *egfp*	In this study
pZE-P3-yveF-yveG-egfp	pZE12-*luc* carrying P$_{padC}$ mutant P3, and *yveF* and *yveG* from *Bacillus subtilis* and *egfp*	In this study
pZE-P4-yveF-yveG-egfp	pZE12-*luc* carrying P$_{padC}$ mutant P4, and *yveF* and *yveG* from *Bacillus subtilis* and *egfp*	In this study
pZE-P5-yveF-yveG-egfp	pZE12-*luc* carrying P$_{padC}$ mutant P5, and *yveF* and *yveG* from *Bacillus subtilis* and *egfp*	In this study
pZE-P6-yveF-yveG-egfp	pZE12-*luc* carrying P$_{padC}$ mutant P6, and *yveF* and *yveG* from *Bacillus subtilis* and *egfp*	In this study
pZE-P7-yveF-yveG-egfp	pZE12-*luc* carrying P$_{padC}$ mutant P7, and *yveF* and *yveG* from *Bacillus subtilis* and *egfp*	In this study
pZE-P8-yveF-yveG-egfp	pZE12-/wc carrying P$_{padC}$ mutant P8, and *yveF* and*yveG* from *Bacillus subtilis* and *egfp*	In this study
pZE-P9-yveF-yveG-egfp	pZE12-*luc* carrying P$_{padC}$ mutant P9, and *yveF* and*yveG* from *Bacillus subtilis* and *egfp*	In this study
pZE-P10-yveF-yveG-egfp	pZE12-*luc* carrying P$_{padC}$ mutant P10, and *yveF* and *yveG* from *Bacillus subtilis* and *egfp*	In this study
pZE-P11-yveF-yveG-egfp	pZE12-*luc* carrying P$_{padC}$ mutant P11, and *yveF* and *yveG* from *Bacillus subtilis* and *egfp*	In this study
pZE-P12-yveF-yveG-egfp	pZE12-*luc* carrying P$_{padC}$ mutant P12, and*yveF* and *yveG* from *Bacillus subtilis* and *egfp*	In this study
pZE-P13-yveF-yveG-egfp	pZE12-*luc* carrying P$_{padC}$ mutant P13, and *yveF* and *yveG* from *Bacillus subtilis* and *egfp*	In this study
pZE-P1-egfp	pZE12-*luc* carrying P$_{padC}$ mutant P1 and *egfp*	In this study
pZE-P2-egfp	pZE12-*luc* carrying P$_{padC}$ mutant P2 and *egfp*	In this study
pZE-P3-egrp	pZE12-*luc* carrying P$_{padC}$ mutant P3 and egfp	In this study
pZE-P4-egfp	pZE12-*luc* carrying P$_{padC}$ mutant P4 and *egfp*	In this study

Author Manuscript

Author Manuscript

Author Manuscript

Author Manuscript

pZE-P5-egfp	pZE12-*luc* carrying P_{padC} mutant P5 and *egfp*	In this study
pZE-P6-egfp	pZE12-*luc* carrying P_{padC} mutant P6 and *egfp*	In this study
pZE-P7-egfp	pZE12-*luc* carrying P_{padC} mutant P7 and *egfp*	In this study
pZE-P8-egfp	pZE12-*luc* carrying P_{padC} mutant P8 and *egfp*	In this study
pZE-P9-egfp	pZE12-*luc* carrying P_{padC} mutant P9 and *egfp*	In this study
pZE-P10-egfp	pZE12-*luc* carrying P_{padC} mutant P10 and *egfp*	In this study
pZE-P11-egfp	pZE12-*luc* carrying P_{padC} mutant P11 and *egfp*	In this study
pZE-P12-egfp	pZE12-*luc* carrying P_{padC} mutant P12 and *egfp*	In this study
pZE-P13-egfp	pZE12-*luc* carrying P_{padC} mutant P13 and *egfp*	In this study
pSC-lpp1.0-yveF-yveG	pCS27 carrying lpp1.0, *yveF*, and *yveG*	In this study

Author Manuscript

Author Manuscript

Author Manuscript

Author Manuscript

Table 2

the sequence of genes and hybrid promoters

Name	Sequence
$\mathbf{P_{padC}}$	GGACTGTCTTCAAACAGTCCTTGTTTTTTTATGTTCCTATTGTTTGACAGT TAACTGCAATGGTGTTAAAGTGAACATGTAAATAGTTACATGATTTTTTC TGAAGGT
yveF	gtgAAGAAGCCGGTTTTAAAACCATTCGCCTCTTTAGAAATCAAGGTTGAT CCGCCTATCACGATTGGTGAGACAAGCCTGGGACTGAGAtga
yveG	atgATTCGCGCTAACGGCAGAACAGATTTATCTGCCAGGTATGTGATTGAA ACAGCAGATCATGAACTGATTTACATTGAAAACAATGGAATACGGCAAG TCAGCAAGCCGTTTCGAAAACAAGCGGCAGCCGGGGAAATTATTGAACC GGAGCATGTTTATTTTCGTACGGTACCGACGTTTGAAACAGGCAGTGAAG TCTATCAATGGCTCCATGACCGCTTGTTTATCGGTTCCGCAGAAAGAACC CCTGATTACGTTCTACTAGACATTTATGAAGTACAGtaa
P1	AACATGTAAATAGTTACATGATtgacaTAAATACCACTGGCGGTgatactGAG CACATCAGCAGGACGCACTGACC
P2	TAAATTATCTCTGGCGGTGttgacaAACATGTAAATAGTTACATGATgatactGA GCACATCAGCAGGACGCACTGACC
P3	AACATGTAAATAGTTACATGATtgacaAACATGTAAATAGTTACATGATgata ctGAGCACATCAGCAGGACGCACTGACC
P4	ATGGTGTTAAAGTGAACATGTAttgacaTAAATACCACTGGCGGTgatactGAG CACATCAGCAGGACGCACTGACC
P5	TAAATTATCTCTGGCGGTGttgacaATGGTGTTAAAGTGAACATGTAgatactGA GCACATCAGCAGGACGCACTGACC
P6	ATGGTGTTAAAGTGAACATGTAttgacaATGGTGTTAAAGTGAACATGTAgata ctGAGCACATCAGCAGGACGCACTGACC
P7	AACATGTAAATAGTTACATGATtgacaATGGTGTTAAAGTGAACATGTAgata ctGAGCACATCAGCAGGACGCACTGACC
P8	ATGGTGTTAAAGTGAACATGTAttgacaAACATGTAAATAGTTACATGATgata ctGAGCACATCAGCAGGACGCACTGACC
P9	TAAATTATCTCTGGCGGTGttgacaTAAATACCACTGGCGGTgatactgAACATGTAAATAGTTACATGAT
P10	TAAATTATCTCTGGCGGTGttgacaTAAATACCACTATGGTGTtaaagtGAACATGTAagcaggacgcactgacc
P11	TAAATTATCTCTGGCGGTGttgacaTAAATACCACTATGGTGTgatactGAACATGTAagcaggacgcactgacc
P12	TAAATTATCTCTGGCGGTGttgacaTAAATACCACATGGTGTtaaagtGAACATGTAAATAGTTACATGAT
P13	TAAATTATCTCTGGCGGTGttgacaTAAATACCACATGGTGTgatactGAACATG TAAATAGTTACATGAT